Journal of Histochemistry & Cytochemistry 2023, Vol. 71(2) 73–86

DOI: 10.1369/00221554231158428
journals.sagepub.com/home/jhc
SAGE

Thioflavin S Staining and Amyloid Formation Are Unique to Mixed Tauopathies

Kimberly L. Fiock, Ryan K. Betters, and Marco M. Hefti
Department of Pathology (KLF, RKB, MMH), Experimental Pathology Graduate Program (KLF, MMH), and Interdisciplinary Neuroscience Graduate Program (RKB), University of Iowa, Iowa City, Iowa; and Iowa Neuroscience Institute, Iowa City, Iowa (KLF, RKB, MMH)

Summary
Tau phosphorylation, aggregation, and toxicity are the main drivers of neurodegeneration in multiple tauopathies, including Alzheimer's disease (AD) and frontotemporal lobar degeneration with tau. Although aggregation and amyloid formation are often assumed to be synonymous, the ability of tau aggregates in different diseases to form amyloids in vivo has not been systematically studied. We used the amyloid dye Thioflavin S to look at tau aggregates in mixed tauopathies such as AD and primary age-related tauopathy, as well as pure 3R or 4R tauopathies such as Pick's disease, progressive supranuclear palsy, and corticobasal degeneration. We found that aggregates of tau protein only form thioflavin-positive amyloids in mixed (3R/4R), but not pure (3R or 4R), tauopathies. Interestingly, neither astrocytic nor neuronal tau pathology was thioflavin-positive in pure tauopathies. As most current positron emission tomography tracers are based on thioflavin derivatives, this suggests that they may be more useful for differential diagnosis than the identification of a general tauopathy. Our findings also suggest that thioflavin staining may have utility as an alternative to traditional antibody staining for distinguishing between tau aggregates in patients with multiple pathologies and that the mechanisms for tau toxicity may differ between different tauopathies. (J Histochem Cytochem 71: 73–86, 2023)

Keywords
Alzheimer's disease, amyloid, FTLD, tau, tauopathy, thioflavin

Introduction

The tau protein is historically known for its role in neurodegenerative diseases but also plays an important role in normal neuronal development and microtubule stabilization throughout the lifespan.[1–4] In the case of disease, hyperphosphorylation of tau causes its detachment from microtubules, increasing unbound tau monomers and leading to misfolding and the formation of toxic tau aggregates.[5,6] These protein aggregates are then able to propagate into neighboring neurons, leading to neurodegeneration.[7,8] This process is the main driver of toxicity in multiple neurodegenerative diseases called tauopathies, including Alzheimer's disease (AD) and frontotemporal lobar degeneration with tau (FTLD-tau).[9]

Although they share a common final pathway, neurodegenerative tauopathies vary widely in the composition and cellular localization of tau aggregates. The two most common types of FTLD-tau, progressive supranuclear palsy (PSP) and corticobasal degeneration (CBD), have both neuronal and glial tau aggregates that consist exclusively of the longer 4R tau isoform. In contrast, Pick's disease (PiD), a rare form of FTLD-tau, consists only of neuronal inclusions of 3R tau called Pick bodies.[10] Tau aggregates in the form of neurofibrillary tangles (NFTs) are present in AD but consist of both the 3R and 4R isoforms. Similarly, primary age-related tauopathy (PART) is characterized by NFTs of both 3R and 4R

Received for publication September 1, 2022; accepted January 30, 2023.

Corresponding Author:
Kimberly L. Fiock, Department of Pathology, University of Iowa, 500 Newton Road, 1157ML, Iowa City, IA 52242, USA.
E-mail: kimberly-fiock@uiowa.edu

tau, with pathology mainly limited to the hippocampus.[11] Recent studies show structural differences between insoluble tau aggregates in these various diseases; however, the drivers of these structures and how they are selective for distinct cell types in different diseases remain unclear.[12]

Binding to thioflavin is commonly used to identify amyloids regardless of whether they are composed of tau, β-amyloid, or other proteins.[13] It is also widely used to validate tau oligomers or fibrils generated in vitro for experimental studies. In addition, many of the tracers used for tau positron emission tomography (PET) imaging are derived from thioflavin and related dyes.[14] The relationship between tau aggregation, amyloid formation, and toxicity, however, remains unclear.[15] While both tau-positive tangles and β-amyloid positive plaques in AD are known to be positive for thioflavin, patterns of thioflavin staining in other tauopathies have not been rigorously studied. The limited existing data are contradictory and predate the modern classification of neurodegenerative tauopathies, making them difficult to interpret.[16–18]

We, therefore, present the first systematic study of amyloids across tauopathies. Our findings show that tau aggregates form a thioflavin-positive amyloid in mixed 3R/4R tauopathies but not in 3R-only or 4R-only tauopathies. We believe that these findings have significant impact on the diagnosis and mechanistic understanding of tau pathologies.

Materials and Methods

Tissue Procurement

Formalin-fixed, paraffin-embedded (FFPE) tissue was obtained from the Iowa NeuroBank Core; Brain Bank for Neurodegenerative Disorders at Mayo Clinic, Jacksonville, FL; Harvard Brain Tissue Resource Center; NIH Brain & Tissue Repository-California; Human Brain & Spinal Fluid Resource Center; VA West Los Angeles Medical Center [supported in part by the National Institutes of Health (NIH) and the U.S. Department of Veterans Affairs]; and the NIH NeuroBioBank at the University of Maryland, Baltimore. Tissue collection at the University of Iowa was approved by the institutional review board (HawkIRB protocol #201706772). All other tissue was received de-identified from the brain banks indicated above, and thus, further review was not required. All methods were conducted in accordance with the relevant guidelines, laws, regulations, and ethical standards of our institution and with the 1964 Helsinki Declaration and its later amendments or comparable ethical standards. Diagnoses were made according to the National Alzheimer's Coordinating Center and other published guidelines.[10,19–22] Case information, and the experiments/figures for which each was used, is summarized in Table 1.

Immunohistochemistry

IHC was performed as previously described.[4] Briefly, 5-μm FFPE tissue sections were placed on charged slides and baked overnight at 70C. A Ventana Benchmark XT was used to perform IHC according to the manufacturer's guidelines. Antigen retrieval was done using CC1 (citric acid buffer) for 1 hr followed by primary antibody incubation with an antiphosphorylated tau (Ser202/Thr205) antibody (AT8, MN1020, RRID: AB_223647; Thermo Fisher Scientific; Waltham, MA, USA) for ~30 min at 1:1000. Slides were visualized on an Olympus BX40 brightfield microscope with an Olympus DP27 camera using CellSens software. All antibodies used for staining [IHC and immunofluorescence (IF)] were previously validated using appropriate positive and negative control tissue and primary cell lines. In addition, these antibodies were separately validated by the University of Iowa Hospitals & Clinics and Clinical Laboratory Improvement Amendments (CLIA)-certified diagnostic immunohistochemistry laboratory.

Combined RNA In Situ Hybridization and Immunofluorescence

RNA in situ hybridization (RNAscope) with IF was performed for FFPE tissue using the 3-plex Multiplex Fluorescent v2 Reagent Kit (cat. no. 323100; ACDBio; Newark, CA, USA) with the C2-MAPT probe (cat. no 408991-C2; ACDBio; Newark, CA, USA) diluted 1:50 in probe diluent (cat. no 300041, ACDBio; Newark, CA, USA) or the C1-MAPT probe (cat. no 408991, ACDBio; Newark, CA, USA) non-diluted according to the manufacturer's instructions. Briefly, 5-μm FFPE tissue sections were baked for 1 hr at 75C, deparaffinized using xylene and ethanol, and treated with H_2O_2 (provided in kit) for 10 min at room temperature. Target retrieval was performed using a steamer for 15 min at 85C, followed by Protease Plus treatment for 30 min at 40C in a HybEZ Oven (ACDBio; Newark, CA, USA). The probe was hybridized for 2 hr at 40C in the HybEZ Oven, and slides were stored in 5× SSC overnight. Amplification and detection were performed the following day according to the manufacturer's instructions using the Cyanine 5 TSA fluorophore (NEL745E001KT; Perkin Elmer; Waltham, MA, USA) at 1:400.

For immunofluorescent labeling, slides were washed with TBST made using 10× TBS (cat no.

Table 1. Case Information.

Case ID	Pathologic Diagnosis	Used in Figure(s)	Age (years)	Sex
#1	Control (cardiovascular disease)	Fig. 3	75	Male
#2	Control (mixed drug intoxication)	Fig. 3, Supplemental Fig. 4	61	Female
#3	Control (pulmonary embolism)	Fig. 2, Fig. 3, Supplemental Fig. 3, Supplemental Fig. 4	61	Male
#4	Control (SARS-CoV-19)	Fig. 5	65	Female
#5	Control (cardiovascular disease)	Fig. 4	54	Male
#6	AD, intermediate ADNC	Fig. 1, Fig. 3, Supplemental Fig. 2	89	Female
#7	AD, intermediate ADNC	Fig. 3	95	Male
#8	AD, high ADNC	Fig. 2, Fig. 3, Fig. 5, Supplemental Fig. 3, Supplemental Fig. 4	58	Female
#9	AD, high ADNC	Supplemental Fig. 4	64	Female
#10	AD, high ADNC	Fig. 4	61	Female
#11	PSP	Supplemental Fig. 4	65	Female
#12	PSP	Supplemental Fig 4	67	Male
#13	PSP	Fig. 2, Fig. 3, Supplemental Fig. 3	68	Male
#14	PSP	Fig. 3, Fig. 4	75	Male
#15	PSP	Fig. 1, Fig. 3, Fig. 5, Supplemental Fig. 2	75	Female
#16	CBD/AGD	Supplemental Fig. 4	55	Male
#17	CBD/AGD	Supplemental Fig. 4	70	Male
#18	CBD	Fig. 4	71	Female
#19	CBD	Fig. 3	72	Female
#20	CBD	Fig. 2, Fig. 3, Supplemental Fig. 3	72	Female
#21	CBD	Fig.1, Fig. 3, Fig. 5, Supplemental Fig. 2	78	Male
#22	PiD	Fig. 2, Fig. 5, Supplemental Fig. 3, Supplemental Fig. 4	79	Male
#23	PiD	Supplemental Fig. 4	79	Female
#24	ALS and PART	Fig. 2, Supplemental Fig. 3	87	Female
#25	PD and PART	Fig. 1, Supplemental Fig. 2	88	Male

Abbreviations: AD, Alzheimer's disease; PSP, progressive supranuclear palsy; CBD, corticobasal degeneration; AGD, argyrophilic grain disease; PiD, Pick's disease; ALS, amyotrophic lateral sclerosis; PD, Parkinson's disease; PART, primary age-related tauopathy.

1706435; Bio-Rad; Hercules, CA, USA) and 0.05% Tween20 (cat no. 9005-64-5; Sigma-Aldrich; Burlington, MA, USA). Slides were blocked in normal goat serum (cat no. 31873; Thermo Fisher; Waltham, MA, USA) with TBS and 0.1% bovine serum albumin (BSA; cat no. 9048-46-86, RPI) for 30 min at room temperature. Primary antibodies for glial fibrillary acid protein (GFAP) (16825-1-AP, RRID: AB_2109646; Proteintech; Rosemont, IL, USA) and AT8 (above) were diluted 1:1000 in TBS + 0.1% BSA, and then incubated for 1.5 hr in a humidified slide chamber at room temperature followed by three TBST washes for 5 min. Goat anti-mouse IgG H&L Alexa Fluor 555 (ab150114, RRID: AB_2687594; Abcam; Cambridge, UK) and goat anti-rabbit IgG H&L Alexa Fluor 488 (ab150077, RRID: AB_2630356; Abcam; Cambridge, UK) were diluted 1:1000 in TBS + 0.1% BSA, and slides were incubated for 30 min in a humidified slide chamber at room temperature. After washing 3× for 2 min in TBST, autofluorescence quenching was carried out using TrueBlack Lipofuscin Autofluorescence Quencher diluted according to the manufacturer's guidelines (23007; Biotium; San Francisco, CA, USA) for 30 sec, followed by 4′,6-diamidino-2-phenylindole (DAPI) and coverslipping with VectaShield Plus antifade mounting medium (H-1900; VectorLabs; Newark, CA, USA). Appropriate controls were run with the 3-plex positive (cat. no. 320861; ACDBio; Newark, CA, USA) and 3-plex negative (cat. no. 320871; ACDBio) control probes for RNAscope, as well as an IF-only control to eliminate false-positive or false-negative results (Supplemental Fig. 1). The MAPT probe was previously validated by our lab.[4]

Thioflavin S Staining

Thioflavin S staining was done in a Coplin jar as previously described with adaptations from Sun et al.[23] and Hefti et al.[24] Briefly, FFPE tissue was cut to 5 μm thickness, mounted on superfrost plus slides (12-550-15; Fisher Scientific; Waltham, MA, USA), baked for 1 hr at 70C, and deparaffinized and rehydrated using a graded series of alcohols (xylene, 50/50 xylene/100% ethanol, 100% ethanol, 95% ethanol, 70% ethanol, 50% ethanol). Slides were washed twice in double distilled water and then pretreated with 0.25% potassium permanganate (P279; Fisher Chemical; Waltham, MA,

USA) and 1% sodium borohydride (S678; Fisher Chemical; Waltham, MA, USA) for 4 min each at room temperature before being placed in 3× PBS for 30 min at 4C to avoid photobleaching. Thioflavin S from Fisher Scientific (AC213150250; Arcos Organics; Geel, Belgium) was diluted in 50% ethanol to make a final concentration of 0.05% thioflavin S and filtered through a 0.2-μm polyethersulfone membrane before use. Based on previous experience in our laboratory, thioflavin is stable in solution at 4C for up to 3 months and was filtered before each subsequent use. Slides were incubated in a non-transparent Coplin jar with 50 ml of thioflavin S for 8 min at room temperature, protected from light. Following thioflavin staining, slides were subjected to two changes of 80% ethanol, washed with distilled water 3×, and soaked in 3× PBS for 30 min at 4C. Slides were rinsed again in distilled water, and then TrueBlack was applied as above before slides were mounted with EverBrite Hardset Mounting Medium with NucSpot 640 (23016-T; Biotium; San Francisco, CA, USA) and coverslipped. It is important to note that the emission peak of thioflavin S is 428 nm, making it difficult to use with a traditional nuclear marker like DAPI. For this reason, we chose to use a mounting medium with a 640 nuclear stain to prevent any overlapping fluorescence.

Thioflavin staining was repeated as above with thioflavin from Santa Cruz Biotechnology; Dallas, TX, USA (sc-391005). Staining was validated on each run with an appropriate positive and negative control, and all slides were imaged within 1 week to avoid fading.

Combined Thioflavin S and Immunofluorescence Staining

Five-μm FFPE tissue was baked for 1 hr in a dry oven at 50–60C before deparaffinization and rehydration in xylene and ethanol (xylene 2×, 100% ethanol 2×, 90% ethanol, 70% ethanol) for 5 min each. Slides were washed in double distilled water for 5 min and then placed in preheated antigen retrieval solution in a Coplin jar in a 90C waterbath (0.514 g sodium citrate, 168 μl Triton X-100, 200 ml water) for 10 min. Slides were allowed to cool at room temperature in the antigen retrieval solution for 20 min and then washed 3× in 1× PBS for 5 min each. Pretreatment with potassium permanganate and sodium borohydride and staining of 0.05% thioflavin were done as above. After the final 3× PBS soak and water rinse, a hydrophobic barrier was drawn (H-4000; VectorLabs; Newark, CA, USA), and slides were blocked in a blocking solution (3% BSA in PBS with 180 μL of Triton X-100) for 1 hr at room temperature in a humidified chamber. Slides were washed in 1× PBS 3× for 5 min each with gentle agitation and then covered with AT8 (above, 1:1000) or GT38 (ab246808, 1:500; Abcam; Cambridge, UK) and GFAP (above, 1:1000) diluted in a blocking solution overnight at 4C in the humidified chamber.

Slides were washed again in 1× PBS (3× 5 min) and then covered with Alexa Fluor 555 (above, 1:1000) and Alexa Fluor 488 (above, 1:1000) diluted in a blocking solution for 1 hr at room temperature in the humidified chamber protected from light. Three PBS washes were performed for 5 min each and then the slides were covered with TrueBlack diluted according to the manufacturer's guidelines as above before being mounted with EverBrite Hardset Mounting Medium with NucSpot 640 (above) and coverslipped.

Imaging

All fluorescent slides were visualized on a Leica SP8 CSU confocal microscope using Leica Las-X software. Thioflavin S was visualized using a DAPI filter cube. Microscopic fields were chosen randomly. Image settings were adjusted to minimize saturated pixels, but due to the broad range of expected staining intensity, it was not possible to eliminate all zero or saturated pixels. Identical settings were used across all images in a given comparison (either qualitative or quantitative). All images in each series were acquired using identical settings.

For RNAscope with IF, resulting images were created using the maximum projection feature in LAS X and adjusted for clarity using the same thresholding settings in LAS X and the same level of settings in Adobe Photoshop. For thioflavin S staining with IF, images were created with the maximum projection feature in LAS X and thresholded to the same settings to diminish autofluorescent background staining due to thioflavin S. No other image manipulation has been done. All figures were made in Adobe Illustrator. Microscopy and image analysis were done blinded to the diagnosis where possible.

Confocal Tile Scanning

Tile scanning for thioflavin-stained 5-μm sections was conducted using the Leica TCS SP8 confocal system (Leica Microsystems) and LAS X imaging software (Leica Microsystems; v.3.5.7.23225). All images were taken using a 40×/1.10 water immersion objective, 8000 Hz (unidirectional) scan speed, 1.1 numerical aperture, 77.2 μm pinhole, and line averaging of 16. EverBrite Hardset Mounting Medium with NucSpot 640 was used as a nuclear stain to ensure consistency in the histological region and focus between slides (638 nm laser line, 3.0% intensity, photomultiplier (PMT) detection of 653–751 nm, and gain of 100). A case with IHC-confirmed

thioflavin-positive staining was used to standardize image acquisition settings prior to tile scanning [405 nm laser line with 1.50% intensity and hybrid detection of 439–512 nm with default gain of 50]. Each slide was manually evaluated for thioflavin positivity before selecting a representative region for further image acquisition. A single image was taken at the center of each region prior to enabling the LAS X Navigator and initiating spiral tile scanning with 2.0% border overlap. The spiral scan was run until 25 total tiles (for a 5 × 5 region, 1133 µm × 1133 µm) were imaged, at which point they were saved together as an "overview" file. Each overview was consolidated using "statistical" mosaic merging to allow for downstream quantitative analysis on a single image file for each slide.

Quantification

Quantification of thioflavin staining was done on full 5 × 5 tile scans for three cases per condition (control, AD, CBD, PSP) by separating the thioflavin channel using Las-X software (Leica) and saving as a TIFF file. The TIFF file was then imported into ImageJ, converted to 8-bit, and then thresholded with a cutoff of 70 (on a scale of 0–255). This cutoff was selected as the minimum required to remove background visible in the negative control cases and was applied identically to all images. This TIFF file was then converted into a matrix and the median intensity calculated across the entire image using a custom MATLAB script (Supplemental Fig. 2). *P* values were assessed using a one-way ANOVA.

Quantification for colocalization of AT8 and thioflavin S was done using the images shown in Fig. 2 in the main text. Images were imported into FIJI and then analyzed using the BIOP JACOP ImageJ plugin with automated thresholding (Otsu) for both images to calculate correlation coefficients (Supplemental Table 1).[25]

Results

Astrocytes With Tau Pathology Do Not Show a Qualitative Change in Tau mRNA Expression

We first used a combination of RNA in situ hybridization (RNAscope) and IF to map tau mRNA expression in GFAP-positive astrocytes from patients with AD, PSP, and CBD compared with a non-tauopathy neurodegenerative control. We found no correlation between astrocytic tau pathology ($AT8^+/GFAP^+$ cells) and increased expression of tau mRNA (Fig. 1). As expected, astrocytes expressed low levels of tau mRNA (yellow dots in main panel and insets), suggesting that astrocytic tau is a result of increased tau uptake rather than astrocytic tau production and that neuronal and glial tau aggregates share a common origin in FTLD-tau.

Tau Aggregates Are Thioflavin-positive in Mixed 3R/4R Tauopathies Only

We then used a combination of thioflavin and IF to determine whether thioflavin staining colocalized with tau pathology in astrocytes. We looked at two cases each of AD, PART, PSP, CBD, PiD, and a non-disease control. Each section was stained with GFAP to mark astrocytes and AT8 to identify tau pathology, combined with thioflavin. As expected, we saw thioflavin-positive NFTs in AD and PART, as well as neuritic plaques in AD (Fig. 2, green in main figure and insets in lower right of each panel). Interestingly, there was no thioflavin staining in any of the FTLD-tau cases (PSP, CBD, PiD) despite obvious tau pathology seen on staining with AT8 (Fig. 2, magenta in main figure and insets in upper right of each panel; Supplementary Table 1).

To rule out a possible confounding effect by the IF protocol, we repeated the experiment on an additional two cases per condition with thioflavin alone and saw identical results (data not shown). We then used large-scale tiled images of three cases per condition (AD, PSP, CBD, and control) to quantify total thioflavin staining (representative images in Fig. 3A with high-powered image in Fig. 3B). We excluded PiD due to its rarity and difficulty in obtaining sufficient cases. We found that, again, all FTLD-tau cases were thioflavin-negative regardless of the tau distribution or burden (Fig. 3A and B). AD cases showed both plaques and morphologically obvious NFTs on thioflavin staining (yellow staining with arrowheads). Quantification of three cases per condition noted above (n=12 patients total) shows a statistically significant difference by ANOVA (Fig. 3C). To confirm this was not batch- or manufacturer-dependent, we also tested a batch of thioflavin from a different manufacturer in an independent cohort of PSP and CBD cases (n=2 per condition) and saw the same results (Supplementary Fig. 3).

Thioflavin S Is an Alternative to AD-specific Antibodies

Next, we wanted to further prove that thioflavin staining serves as an alternative to AD-specific antibodies. We tested cortex using the AD tau conformation-specific antibody GT38 paired with thioflavin and GFAP in control, AD, PSP, and CBD cases (n=1 per condition). We found that thioflavin (green) colocalized with GT38 staining (magenta) in NFTs in AD, and both thioflavin and GT38 were negative in all other cases (Fig. 4).

Thioflavin Positivity Does Not Vary Across Regions

To determine whether thioflavin staining is region-specific, we tested the three regions most commonly

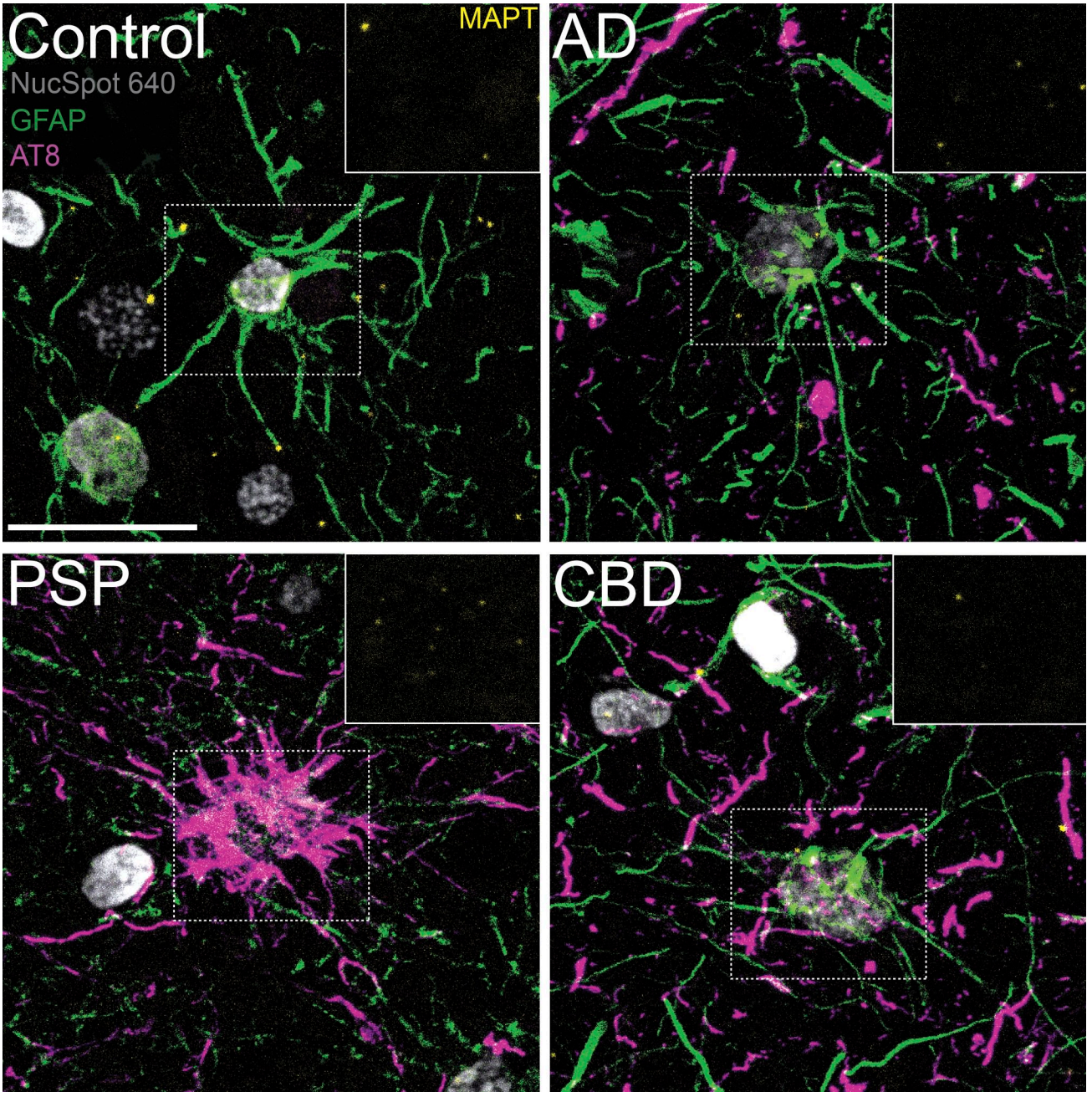

Figure 1. Astrocytes with tau pathology do not express higher levels of tau mRNA. Astrocytes express low levels of tau mRNA (*MAPT*, yellow) that does not qualitatively correlate with tau protein burden (magenta) across all conditions. The insets show the tau mRNA channel from the center of each cell (shown within white, dashed box). NucSpot 640 is shown in gray to highlight nuclei. Some nuclei may appear white due to higher levels of chromatin, such as oligodendrocytes. Scale bar = 50 μm. One case is shown per disease (total n=4). Abbreviations: GFAP, glial fibrillary acidic protein; AT8, phosphorylated tau Ser202/Thr205; MAPT, microtubule associate protein tau; AD, Alzheimer's disease; PSP, progressive supranuclear palsy; CBD, corticobasal degeneration.

affected by tau pathology in AD, PSP, CBD, and PiD cases compared with a non-disease control (n=1 per condition). We included frontal cortex, hippocampus, and substantia nigra (midbrain) for AD and control, whereas PSP, CBD, and PiD were tested in frontal cortex, basal ganglia, and substantia nigra (midbrain). Consistent with our other findings, all regions were negative for thioflavin (green) across all FTLD-tau cases (Fig. 5). Together, this shows that thioflavin staining is not region-dependent and further supports

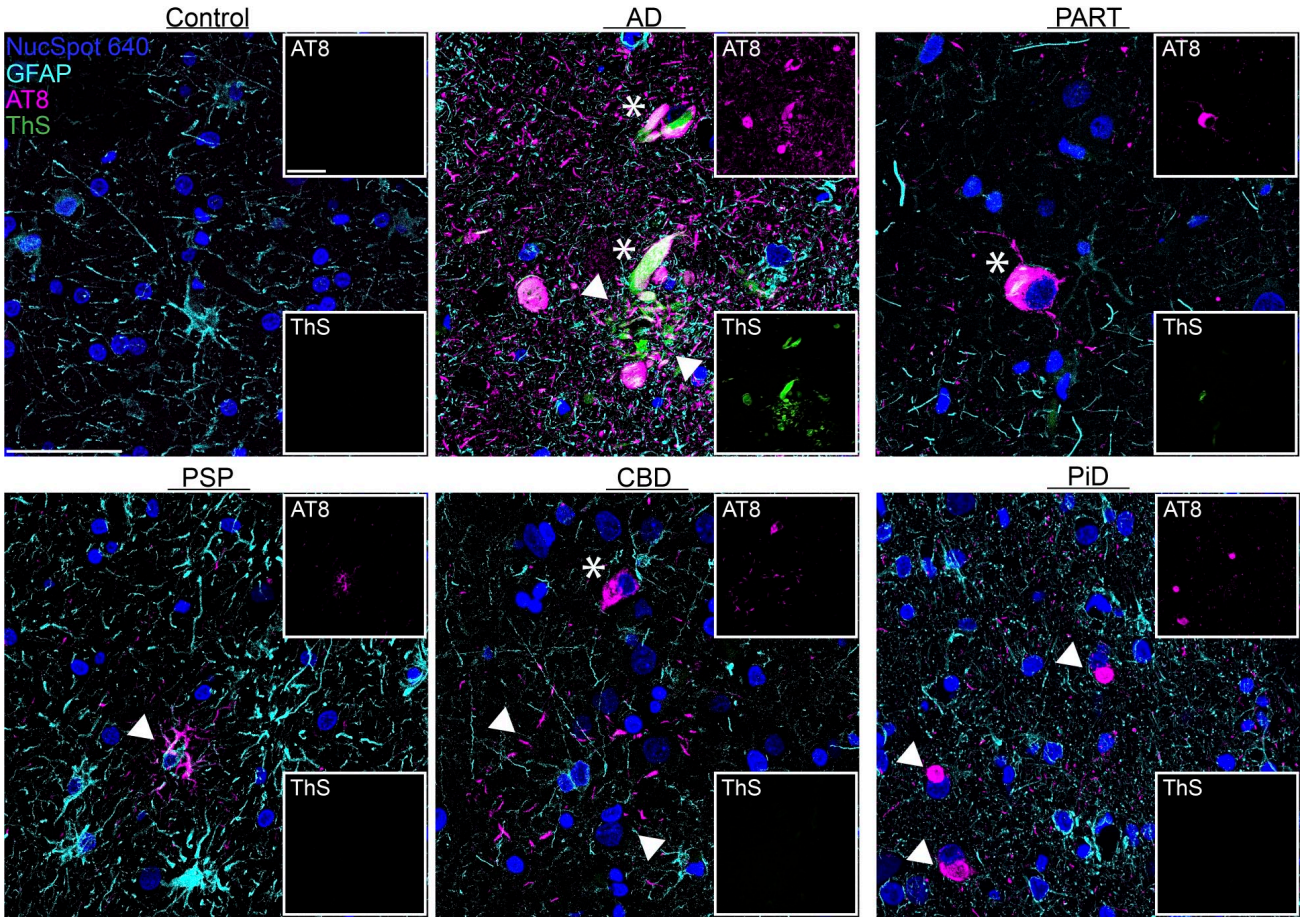

Figure 2. Thioflavin S staining does not colocalize with tau in FTLD-tau. Both tangles (asterisks) and plaques (arrowheads) show ThS and tau colocalization in AD. PART also shows ThS-positive tangles (asterisk). ThS staining is not present in PSP's tufted astrocytes (arrowhead) or CBD's tangles (asterisk) and astrocytic plaques (between arrowheads). Pick bodies (arrowheads) are also ThS-negative. Insets show reduced size views of the entire panel with the indicated channel for clarity. NucSpot 640 is shown in dark blue to highlight nuclei. One case is shown per disease (total n=6). Scale bars = 50 μm. Abbreviations: FTLD-tau, frontotemporal lobar degeneration with tau; GFAP, glial fibrillary acidic protein; AT8, phosphorylated tau Ser202/Thr205; ThS, thioflavin S; AD, Alzheimer's disease; PART, primary age-related tauopathy; PSP, progressive supranuclear palsy; CBD, corticobasal degeneration; PiD, Pick's disease.

our data that tau in 3R-only or 4R-only tauopathies may not be an amyloid.

Discussion

In this study, we demonstrated that neuronal and astrocytic tau in FTLD-tau does not form a thioflavin-positive amyloid, regardless of the region or tau burden, suggesting that pure 3R or 4R tauopathies may be formed by a distinct non-amyloidogenic pathway. Combined with our RNA expression data, this also supports a common origin for neuronal and astrocytic tau in FTLD-tau.

The definition of the term amyloid, and therefore the criteria for calling a particular protein aggregate an amyloid, has long been problematic. The latest guidelines from the International Society of Amyloidosis distinguish between an amyloid fibril, which is defined as any cross β-sheet structure, and the medical term amyloid, which is most commonly defined as any pathological material showing appropriate staining patterns with Congo red and/or thioflavin.[26] In the present work, we use the latter, medical, definition. Although we acknowledge that based on structural cryo-electron microscopy studies both pure 3R or 4R and mixed tau fibrils meet the chemical definition of an amyloid by having a cross beta-sheet structure, our data strongly suggest that there are fundamental differences in packing density and structure, and that FTLD-tau does not meet the conventional medical definition of an amyloid.[12] This is of more than semantic importance because, as discussed in more detail below, thioflavin and its derivatives are used for tau PET scanning and as a readout for aggregation in preparing recombinant tau oligomers and fibrils.

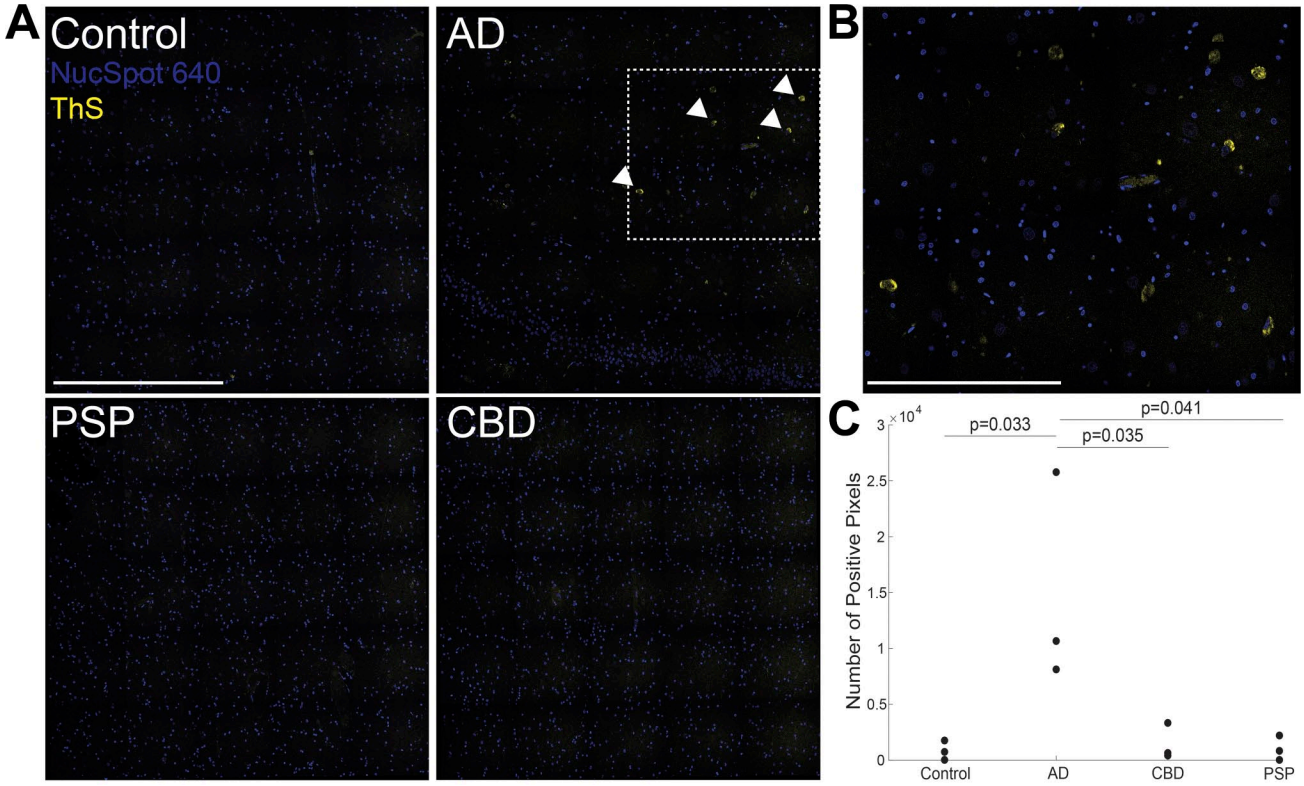

Figure 3. Quantification of thioflavin S staining shows a significant difference between AD and FTLD-tau. Images have two channels with NucSpot 640 shown in blue to highlight nuclei and thioflavin S shown in yellow. (A) 232.5 μm × 232.5 μm tiled images stitched together (1133 μm × 1133 μm total) reveal thioflavin staining in AD (arrowheads) but not in PSP or CBD. The full 5 × 5 tiled image is shown. (B) Inset of AD case highlights thioflavin-positive staining. White, dashed box represents the area from which the inset was taken in the full tiled image. Panels A and B show representative images from the 12 cases (n=3 per disease, total n=12) analyzed in panel C. (C) Quantification shows AD has significantly higher amounts of thioflavin-positive staining compared with control, PSP, or CBD (one-way ANOVA). For statistical analysis, each point represents an individual patient with the indicated disease (or non-disease control), for a total of three cases per disease (total n=12). The entire titled image was quantified for each patient. Scale bar = 500 μm in main panel, 250 μm in inset. Abbreviations: AD, Alzheimer's disease; FTLD-tau, frontotemporal lobar degeneration with tau; PSP, progressive supranuclear palsy; CBD, corticobasal degeneration.

The existing data on thioflavin staining as a measure of amyloid formation in FTLD-tau are limited. Rare case reports have shown thioflavin-positive NFTs in the dentate gyrus of patients with PSP but do not describe astrocytic pathology.[16,17] Consistent with our findings, a single study of cortical NFTs in CBD showed a lack of thioflavin staining.[18] Another study reported staining in globose tangles, but not astrocytes, of PSP patients, but was limited to sections of midbrain. In this same study, CBD showed no thioflavin-positive staining in the neocortex.[27] These studies are difficult to interpret, however, in that the majority predates the first description of PART, which can co-occur with FTLD-tau and would lead to mixed, rather than pure, 4R tau aggregates in the hippocampal formation and/or brainstem.[11,28] One recent study showed thioflavin-positive staining in a Pick body in Pick's disease and in a coiled body in PSP,[29] which was not seen in our study. Two possible explanations for the discrepancy with our current study are differences in thioflavin S concentration used and the small sample size in Koga et al.[29]

There has been significant progress in developing alternative fluorescent amyloid markers derived from Congo red or aminonaphthalene. Some of these markers [e.g., (trans, trans)-1-bromo-2,5-bis-(3-hydroxycarbonyl-4-hydroxy)styrylbenzene (BSB), (trans,trans)-1-fluoro-2,5-bis(3-hydroxycarbonyl-4-hydroxy)styrylbenzene (FSB)] do appear to stain tau pathology in PSP or CBD, whereas others, such as 2-(1-{6-[(2-[F-18]fluoroethyl) (methyl)amino]-2-naphthyl} ethylidene) malononitrile (FDDNP), do not.[27,30,31] As above, these studies predate the modern classification system used to describe neurodegenerative diseases, so a concurrent diagnosis of PART cannot be excluded. There are even less data looking at more recently described

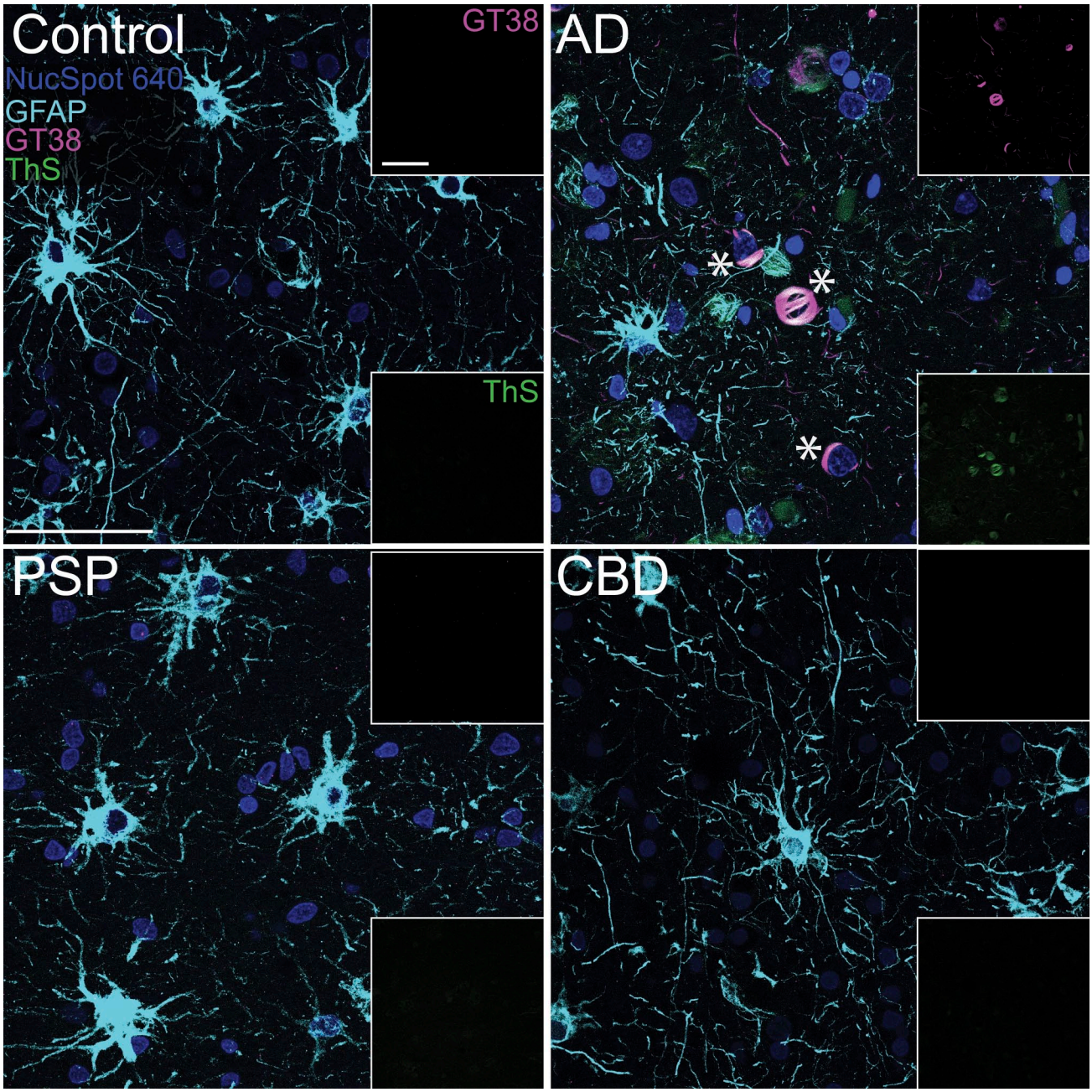

Figure 4. Thioflavin S staining colocalizes with conformation-specific tau antibody GT38. Tangles show ThS (green) and GT38 (magenta) colocalization in AD, evidenced by a white overlay (asterisks). No ThS or GT38 staining is present in control, PSP, or CBD. NucSpot 640 is shown in dark blue to highlight nuclei. One case is shown per disease (total n=4). Scale bar = 50 μm for both the main image and inset. Abbreviations: GFAP, glial fibrillary acidic protein; GT38, conformation-specific AD tau; ThS, thioflavin S; AD, Alzheimer's disease; PSP, progressive supranuclear palsy; CBD, corticobasal degeneration.

tauopathies, such as chronic traumatic encephalopathy (CTE) and PART. A single study looking at CTE showed thioflavin staining in diffuse plaques, presumably representing concurrent AD, but positive staining in tau aggregates was not reported.[32] Our findings are in agreement with recently published data showing that conformation-specific anti-tau antibodies can distinguish between AD and FTLD-tau aggregates in postmortem human brain.[33,34]

Our results have several potential scientific implications. Recent data suggest that there is a high degree of concurrent neurodegenerative diseases in the

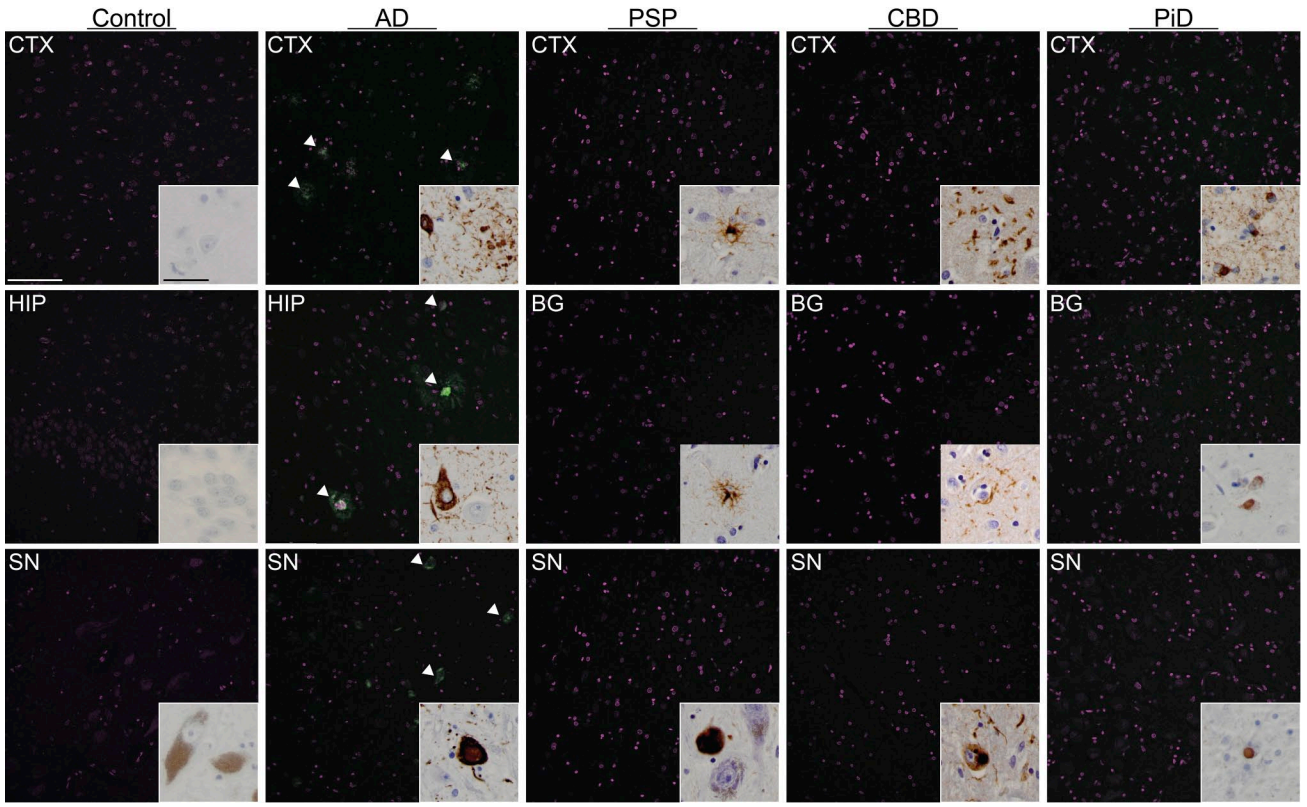

Figure 5. Lack of thioflavin S staining in FTLD-tau is not region-specific. Thioflavin staining (green) is present in all regions of AD (arrowheads) but is not found in any regions of control, PSP, CBD, or PiD. NucSpot 640 is shown in magenta to highlight nuclei. Insets show tau staining (AT8) in the same area despite no thioflavin positivity. One case is shown per disease, with three regions per case (total n=5). White scale bar = 100 μm, black scale bar = 50 μm. Abbreviations: FTLD-tau, frontotemporal lobar degeneration with tau; CTX, cortex; HIP, hippocampus; SN, substantia nigra; BG, basal ganglia; AD, Alzheimer's disease; PSP, progressive supranuclear palsy; CBD, corticobasal degeneration; PiD, Pick's disease.

aging brain.[35–37] Based on our results, thioflavin staining may be a simple method to distinguish concurrent FTLD-tau and AD pathology, particularly in the brainstem and/or in the early stages of both diseases. For example, tau-positive dystrophic neurites in a neuritic plaque in AD may be difficult to distinguish from an astrocyte plaque in CBD using the diagnostic marker AT8, especially if both diseases are present. Use of a readily available and simple stain has significant advantages over use of tau-isoform-specific antibodies (e.g., RD3, RD4), although ideally both would be used for greater rigor.

PET imaging has become one of the leading methods for neurodegenerative disease diagnosis. PET ligand ^{18}F-flortaucipir (AV-1451) binding to tau fibrils in AD has been well characterized, but its use in FTLD-tau has been more uncertain.[38–41] In addition, a study looking at ^{18}F-flortaucipir in CTE showed limited success.[42] Because ^{18}F-flortaucipir is a thioflavin S derivative, our data suggest that it may be problematic for detection of tau pathology in tauopathies other than AD but may be extremely useful for differential diagnosis, in that a patient with a strong tau-PET signal is more likely to have a mixed tauopathy. The different staining characteristics of individual fluorescent dyes raise the intriguing possibility that a combination of PET markers may be able to diagnose specific neurodegenerative tauopathies by characterizing tau aggregate structures in vitro. Thioflavin is also used as a readout when preparing recombinant tau seeds for in vivo or studies. Our data, combined with recent structural studies showing significant differences between recombinant and brain-derived tau aggregates, suggest that this approach may be problematic.[43]

The implications of our work clinically are less clear. Because fluorescent microscopy is not a portion of the routine diagnostic workflow, and the application of fluorescent microscopy requires specialized reagents and equipment, our study is not sufficient to establish clinical utility of this method in a diagnostic laboratory. It does, however, suggest that additional studies are warranted. Introduction of a novel stain

and imaging approach would require substantial validation for performance within a CLIA laboratory setting (or another analogous diagnostic accreditation setting such as College of American Pathologists (CAP) accreditation). Future studies should include a statistically determined number of samples from multiple sources across different laboratories to ensure reproducibility of the results.

Due to limitations in sample availability, we were unable to fully characterize PiD and did not explore amyloid formation in CTE. Further research with a larger sampling of these diseases and a focus on tau pathology is necessary to obtain a full understanding of amyloid formation. Our study is also limited by its observational nature, and further mechanistic studies will be required to confirm the hypothesis that this is driven by the relative ratios of 3R and 4R tau pathology. Because it is the best characterized and most reliable stain for amyloids in postmortem human brain tissue, we focused on thioflavin S, rather than using Congo red that has nonspecific staining of native proteins or other less well-characterized dyes.[44,45] Future research identifying other methods of amyloid detection may be useful in supporting our data, in addition to structural studies addressing how thioflavin interacts with individual tau structures.

Our study is the first to address amyloid formation in non-AD tauopathies. The findings clarify the distinction between an amyloid and an aggregate, highlighting that these terms are not interchangeable because not all aggregates may be true amyloids. The data suggest significant variability among tauopathies in the formation and toxicity of tau aggregates and point to the need to more precisely define tau-related diagnostic tools.

Acknowledgments

The authors would like to thank Ms. Mariah Leidinger and the University of Iowa Comparative Pathology Laboratory for their histology and tissue processing services, and Steven Moore, MD, PhD, Michael Dailey, PhD, and Franz Hefti, PhD for their critical reading of the manuscript. They would also like to acknowledge the incredible contribution of the patient donors and their families, as this research would not be possible without their generous gift to the advancement of science, as well as the support staff at the University of Iowa who worked tirelessly behind the scenes to keep our facilities running.

Competing Interests

The author(s) declared no potential conflicts of interest with respect to the research, authorship, and/or publication of this article.

Author Contributions

KLF and MMH contributed to the study conception and design. Data collection was performed by KLF and RKB. Data analysis was done by MMH. The first draft of the manuscript was written by KLF and MMH. All authors read and approved the final manuscript.

Funding

The author(s) disclosed receipt of the following financial support for the research, authorship, and/or publication of this article: This work was funded by grants from the National Institutes of Health (K23NS109284), the Roy J. Carver Foundation, and the Carver College of Medicine at the University of Iowa, all to M.M.H.; a Cornerstone Grant from the Histochemical Society to K.L.F.; and the Kwak-Ferguson Fellowship to R.K.B.

ORCID iD

Marco M. Hefti https://orcid.org/0000-0002-3127-4528

Data Accessibility Statement

All data not included in the paper are available upon reasonable request to the corresponding author. MATLAB code is available in Supplementary Fig. 1.

Supplemental Material

Supplemental material for this article is available online.

Literature Cited

1. Shahani N, Brandt R. Functions and malfunctions of the tau proteins. Cell Mol Life Sci. 2002;59(10):1668–80. doi:10.1007/pl00012495.
2. Sennvik K, Boekhoorn K, Lasrado R, Terwel D, Verhaeghe S, Korr H, Schmitz C, Tomiyama T, Mori H, Krugers H, Joels M, Ramakers GJ, Lucassen PJ, Van Leuven F. Tau-4R suppresses proliferation and promotes neuronal differentiation in the hippocampus of tau knockin/knockout mice. FASEB J. 2007;21(9):2149–61. doi:10.1096/fj.06-7735com.
3. Dawson HN, Ferreira A, Eyster MV, Ghoshal N, Binder LI, Vitek MP. Inhibition of neuronal maturation in primary hippocampal neurons from tau deficient mice. J Cell Sci. 2001;114(Pt 6):1179–87.
4. Fiock KL, Smalley ME, Crary JF, Pasca AM, Hefti MM. Increased tau expression correlates with neuronal maturation in the developing human cerebral cortex. eNeuro. 2020;7:ENEURO.0058-20.2020. doi:10.1523/ENEURO.0058-20.2020.
5. Ward SM, Himmelstein DS, Lancia JK, Binder LI. Tau oligomers and tau toxicity in neurodegenerative disease. Biochem Soc Trans. 2012;40(4):667–71. doi:10.1042/BST20120134.
6. Lasagna-Reeves CA, Castillo-Carranza DL, Sengupta U, Sarmiento J, Troncoso J, Jackson GR, Kayed R.

Identification of oligomers at early stages of tau aggregation in Alzheimer's disease. FASEB J. 2012;26(5):1946–59. doi:10.1096/fj.11-199851.
7. He Z, Guo JL, McBride JD, Narasimhan S, Kim H, Changolkar L, Zhang B, Gathagan RJ, Yue C, Dengler C, Stieber A, Nitla M, Coulter DA, Abel T, Brunden KR, Trojanowski JQ, Lee VM. Amyloid-beta plaques enhance Alzheimer's brain tau-seeded pathologies by facilitating neuritic plaque tau aggregation. Nat Med. 2018;24(1):29–38. doi:10.1038/nm.4443.
8. Falcon B, Cavallini A, Angers R, Glover S, Murray TK, Barnham L, Jackson S, O'Neill MJ, Isaacs AM, Hutton ML, Szekeres PG, Goedert M, Bose S. Conformation determines the seeding potencies of native and recombinant Tau aggregates. J Biol Chem. 2015;290(2):1049–65. doi:10.1074/jbc.M114.589309.
9. Morris M, Maeda S, Vossel K, Mucke L. The many faces of tau. Neuron. 2011;70(3):410–26. doi:10.1016/j.neuron.2011.04.009.
10. Dickson DW, Kouri N, Murray ME, Josephs KA. Neuropathology of frontotemporal lobar degeneration-tau (FTLD-tau). J Mol Neurosci. 2011;45(3):384–9. doi:10.1007/s12031-011-9589-0.
11. Crary JF, Trojanowski JQ, Schneider JA, Abisambra JF, Abner EL, Alafuzoff I, Arnold SE, Attems J, Beach TG, Bigio EH, Cairns NJ, Dickson DW, Gearing M, Grinberg LT, Hof PR, Hyman BT, Jellinger K, Jicha GA, Kovacs GG, Knopman DS, Kofler J, Kukull WA, Mackenzie IR, Masliah E, McKee A, Montine TJ, Murray ME, Neltner JH, Santa-Maria I, Seeley WW, Serrano-Pozo A, Shelanski ML, Stein T, Takao M, Thal DR, Toledo JB, Troncoso JC, Vonsattel JP, White CL 3rd, Wisniewski T, Woltjer RL, Yamada M, Nelson PT. Primary age-related tauopathy (PART): a common pathology associated with human aging. Acta Neuropathol. 2014;128(6):755–66. doi:10.1007/s00401-014-1349-0.
12. Shi Y, Zhang W, Yang Y, Murzin AG, Falcon B, Kotecha A, van Beers M, Tarutani A, Kametani F, Garringer HJ, Vidal R, Hallinan GI, Lashley T, Saito Y, Murayama S, Yoshida M, Tanaka H, Kakita A, Ikeuchi T, Robinson AC, Mann DMA, Kovacs GG, Revesz T, Ghetti B, Hasegawa M, Goedert M, Scheres SHW. Structure-based classification of tauopathies. Nature. 2021;598(7880):359–63. doi:10.1038/s41586-021-03911-7.
13. Dickson DW. Required techniques and useful molecular markers in the neuropathologic diagnosis of neurodegenerative diseases. Acta Neuropathol. 2005;109(1):14–24. doi:10.1007/s00401-004-0950-z.
14. Mathis CA, Lopresti BJ, Ikonomovic MD, Klunk WE. Small-molecule PET tracers for imaging proteinopathies. Semin Nucl Med. 2017;47(5):553–75. doi:10.1053/j.semnuclmed.2017.06.003.
15. Chiti F, Dobson CM. Protein misfolding, amyloid formation, and human disease: a summary of progress over the last decade. Annu Rev Biochem. 2017;86:27–68. doi:10.1146/annurev-biochem-061516-045115.
16. Wakabayashi K, Hansen LA, Vincent I, Mallory M, Masliah E. Neurofibrillary tangles in the dentate granule cells of patients with Alzheimer's disease, Lewy body disease and progressive supranuclear palsy. Acta Neuropathol. 1997;93(1):7–12. doi:10.1007/s004010050576.
17. Hof PR, Delacourte A, Bouras C. Distribution of cortical neurofibrillary tangles in progressive supranuclear palsy: a quantitative analysis of six cases. Acta Neuropathol. 1992;84(1):45–51. doi:10.1007/BF00427214.
18. Uchihara T, Mitani K, Mori H, Kondo H, Yamada M, Ikeda K. Abnormal cytoskeletal pathology peculiar to corticobasal degeneration is different from that of Alzheimer's disease or progressive supranuclear palsy. Acta Neuropathol. 1994;88(4):379–83. doi:10.1007/BF00310383.
19. Armstrong MJ, Litvan I, Lang AE, Bak TH, Bhatia KP, Borroni B, Boxer AL, Dickson DW, Grossman M, Hallett M, Josephs KA, Kertesz A, Lee SE, Miller BL, Reich SG, Riley DE, Tolosa E, Troster AI, Vidailhet M, Weiner WJ. Criteria for the diagnosis of corticobasal degeneration. Neurology. 2013;80(5):496–503. doi:10.1212/WNL.0b013e31827f0fd1.
20. Dickson DW, Bergeron C, Chin SS, Duyckaerts C, Horoupian D, Ikeda K, Jellinger K, Lantos PL, Lippa CF, Mirra SS, Tabaton M, Vonsattel JP, Wakabayashi K, Litvan I; Office of Rare Diseases of the National Institutes of Health. Office of Rare Diseases neuropathologic criteria for corticobasal degeneration. J Neuropathol Exp Neurol. 2002;61(11):935–46. doi:10.1093/jnen/61.11.935.
21. Hoglinger GU, Respondek G, Stamelou M, Kurz C, Josephs KA, Lang AE, Mollenhauer B, Muller U, Nilsson C, Whitwell JL, Arzberger T, Englund E, Gelpi E, Giese A, Irwin DJ, Meissner WG, Pantelyat A, Rajput A, van Swieten JC, Troakes C, Antonini A, Bhatia KP, Bordelon Y, Compta Y, Corvol JC, Colosimo C, Dickson DW, Dodel R, Ferguson L, Grossman M, Kassubek J, Krismer F, Levin J, Lorenzl S, Morris HR, Nestor P, Oertel WH, Poewe W, Rabinovici G, Rowe JB, Schellenberg GD, Seppi K, van Eimeren T, Wenning GK, Boxer AL, Golbe LI, Litvan I; Movement Disorder Society-endorsed PSP Study Group. Clinical diagnosis of progressive supranuclear palsy: the movement disorder society criteria. Mov Disord. 2017;32(6):853–64. doi:10.1002/mds.26987.
22. Montine TJ, Phelps CH, Beach TG, Bigio EH, Cairns NJ, Dickson DW, Duyckaerts C, Frosch MP, Masliah E, Mirra SS, Nelson PT, Schneider JA, Thal DR, Trojanowski JQ, Vinters HV, Hyman BT; National Institute on Aging; Alzheimer's Association. National Institute on Aging-Alzheimer's Association guidelines for the neuropathologic assessment of Alzheimer's disease: a practical approach. Acta Neuropathol. 2012;123(1):1–11. doi:10.1007/s00401-011-0910-3.
23. Sun A, Nguyen XV, Bing G. Comparative analysis of an improved thioflavin-s stain, Gallyas silver stain, and immunohistochemistry for neurofibrillary tangle demonstration on the same sections. J Histochem Cytochem. 2002;50(4):463–72. doi:10.1177/00221554020500403.
24. Hefti MM, Kim S, Bell AJ, Betters RK, Fiock KL, Iida MA, Smalley ME, Farrell K, Fowkes ME, Crary JF. Tau phos-

phorylation and aggregation in the developing human brain. J Neuropathol Exp Neurol. 2019;78(10):930–8. doi:10.1093/jnen/nlz073.
25. Dunn KW, Kamocka MM, McDonald JH. A practical guide to evaluating colocalization in biological microscopy. Am J Physiol Cell Physiol. 2011;300(4):C723–42. doi:10.1152/ajpcell.00462.2010.
26. Benson MD, Buxbaum JN, Eisenberg DS, Merlini G, Saraiva MJM, Sekijima Y, Sipe JD, Westermark P. Amyloid nomenclature 2018: recommendations by the International Society of Amyloidosis (ISA) nomenclature committee. Amyloid. 2018;25(4):215–9. doi:10.1080/13506129.2018.1549825.
27. Schmidt ML, Schuck T, Sheridan S, Kung MP, Kung H, Zhuang ZP, Bergeron C, Lamarche JS, Skovronsky D, Giasson BI, Lee VM, Trojanowski JQ. The fluorescent Congo red derivative, (trans, trans)-1-bromo-2,5-bis-(3-hydroxycarbonyl-4-hydroxy)styrylbenzene (BSB), labels diverse beta-pleated sheet structures in postmortem human neurodegenerative disease brains. Am J Pathol. 2001;159(3):937–43. doi:10.1016/s0002-9440(10)61769-5.
28. Kovacs GG, Lukic MJ, Irwin DJ, Arzberger T, Respondek G, Lee EB, Coughlin D, Giese A, Grossman M, Kurz C, McMillan CT, Gelpi E, Compta Y, van Swieten JC, Laat LD, Troakes C, Al-Sarraj S, Robinson JL, Roeber S, Xie SX, Lee VM, Trojanowski JQ, Hoglinger GU. Distribution patterns of tau pathology in progressive supranuclear palsy. Acta Neuropathol. 2020;140(2):99–119. doi:10.1007/s00401-020-02158-2.
29. Koga S, Ono M, Sahara N, Higuchi M, Dickson DW. Fluorescence and autoradiographic evaluation of tau PET ligand PBB3 to alpha-synuclein pathology. Mov Disord. 2017;32(6):884–92. doi:10.1002/mds.27013.
30. Smid LM, Vovko TD, Popovic M, Petric A, Kepe V, Barrio JR, Vidmar G, Bresjanac M. The 2,6-disubstituted naphthalene derivative FDDNP labeling reliably predicts Congo red birefringence of protein deposits in brain sections of selected human neurodegenerative diseases. Brain Pathol. 2006;16(2):124–30. doi:10.1111/j.1750-3639.2006.00006.x.
31. Velasco A, Fraser G, Delobel P, Ghetti B, Lavenir I, Goedert M. Detection of filamentous tau inclusions by the fluorescent Congo red derivative FSB [(trans, trans)-1-fluoro-2,5-bis(3-hydroxycarbonyl-4-hydroxy)styrylbenzene]. FEBS Lett. 2008;582(6):901–6. doi:10.1016/j.febslet.2008.02.025.
32. Kelley CM, Perez SE, Mufson EJ. Tau pathology in the medial temporal lobe of athletes with chronic traumatic encephalopathy: a chronic effects of neurotrauma consortium study. Acta Neuropathol Commun. 2019;7(1):207. doi:10.1186/s40478-019-0861-9.
33. Gibbons GS, Kim SJ, Robinson JL, Changolkar L, Irwin DJ, Shaw LM, Lee VM, Trojanowski JQ. Detection of Alzheimer's disease (AD) specific tau pathology with conformation-selective anti-tau monoclonal antibody in co-morbid frontotemporal lobar degeneration-tau (FTLD-tau). Acta Neuropathol Commun. 2019;7(1):34. doi:10.1186/s40478-019-0687-5.
34. Gibbons GS, Banks RA, Kim B, Changolkar L, Riddle DM, Leight SN, Irwin DJ, Trojanowski JQ, Lee VMY. Detection of Alzheimer disease (AD)-specific tau pathology in AD and NonAD tauopathies by immunohistochemistry with novel conformation-selective tau antibodies. J Neuropathol Exp Neurol. 2018;77(3):216–28. doi:10.1093/jnen/nly010.
35. Spires-Jones TL, Attems J, Thal DR. Interactions of pathological proteins in neurodegenerative diseases. Acta Neuropathol. 2017;134(2):187–205. doi:10.1007/s00401-017-1709-7.
36. Armstrong RA, Lantos PL, Cairns NJ. Overlap between neurodegenerative disorders. Neuropathology. 2005;25(2):111–24. doi:10.1111/j.1440-1789.2005.00605.x.
37. Robinson JL, Lee EB, Xie SX, Rennert L, Suh E, Bredenberg C, Caswell C, Van Deerlin VM, Yan N, Yousef A, Hurtig HI, Siderowf A, Grossman M, McMillan CT, Miller B, Duda JE, Irwin DJ, Wolk D, Elman L, McCluskey L, Chen-Plotkin A, Weintraub D, Arnold SE, Brettschneider J, Lee VM, Trojanowski JQ. Neurodegenerative disease concomitant proteinopathies are prevalent, age-related and APOE4-associated. Brain. 2018;141(7):2181–93. doi:10.1093/brain/awy146.
38. Lowe VJ, Curran G, Fang P, Liesinger AM, Josephs KA, Parisi JE, Kantarci K, Boeve BF, Pandey MK, Bruinsma T, Knopman DS, Jones DT, Petrucelli L, Cook CN, Graff-Radford NR, Dickson DW, Petersen RC, Jack CR Jr, Murray ME. An autoradiographic evaluation of AV-1451 Tau PET in dementia. Acta Neuropathol Commun. 2016;4(1):58. doi:10.1186/s40478-016-0315-6.
39. Marquie M, Normandin MD, Meltzer AC, Siao Tick Chong M, Andrea NV, Anton-Fernandez A, Klunk WE, Mathis CA, Ikonomovic MD, Debnath M, Bien EA, Vanderburg CR, Costantino I, Makaretz S, DeVos SL, Oakley DH, Gomperts SN, Growdon JH, Domoto-Reilly K, Lucente D, Dickerson BC, Frosch MP, Hyman BT, Johnson KA, Gomez-Isla T. Pathological correlations of [F-18]-AV-1451 imaging in non-alzheimer tauopathies. Ann Neurol. 2017;81(1):117–28. doi:10.1002/ana.24844.
40. Sander K, Lashley T, Gami P, Gendron T, Lythgoe MF, Rohrer JD, Schott JM, Revesz T, Fox NC, Arstad E. Characterization of tau positron emission tomography tracer [(18)F]AV-1451 binding to postmortem tissue in Alzheimer's disease, primary tauopathies, and other dementias. Alzheimers Dement. 2016;12(11):1116–24. doi:10.1016/j.jalz.2016.01.003.
41. Tsai RM, Bejanin A, Lesman-Segev O, LaJoie R, Visani A, Bourakova V, O'Neil JP, Janabi M, Baker S, Lee SE, Perry DC, Bajorek L, Karydas A, Spina S, Grinberg LT, Seeley WW, Ramos EM, Coppola G, Gorno-Tempini ML, Miller BL, Rosen HJ, Jagust W, Boxer AL, Rabinovici GD. (18)F-flortaucipir (AV-1451) tau PET in frontotemporal dementia syndromes. Alzheimers Res Ther. 2019;11(1):13. doi:10.1186/s13195-019-0470-7.
42. Marquie M, Aguero C, Amaral AC, Villarejo-Galende A, Ramanan P, Chong MST, Saez-Calveras N, Bennett RE, Verwer EE, Kim SJW, Dhaynaut M, Alvarez VE, Johnson KA, McKee AC, Frosch MP, Gomez-Isla T. [(18)F]-AV-

1451 binding profile in chronic traumatic encephalopathy: a postmortem case series. Acta Neuropathol Commun. 2019;7(1):164. doi:10.1186/s40478-019-0808-1.
43. Zhang W, Falcon B, Murzin AG, Fan J, Crowther RA, Goedert M, Scheres SH. Heparin-induced tau filaments are polymorphic and differ from those in Alzheimer's and Pick's diseases. Elife. 2019;8. doi:10.7554/eLife.43584.
44. Khurana R, Uversky VN, Nielsen L, Fink AL. Is Congo red an amyloid-specific dye? J Biol Chem. 2001;276(25): 22715–21. doi:10.1074/jbc.M011499200.
45. Yakupova EI, Bobyleva LG, Vikhlyantsev IM, Bobylev AG. Congo Red and amyloids: history and relationship. Biosci Rep. 2019;39(1):BSR20181415. doi:10.1042/BSR20181415.